IJMMS, Vol. 13, No. 1, (January-June 2017):59-72

ISSN: 0973-3329

EFFECTS OF HOMOGENOUS-HETEROGENOUS REACTIONS ON ELECTRICALLY CONDUCTING POWELL-ERYING FLUID WITH VARIABLE SUCTION OR INJECTION

P. Suresh*, N.L Bhikshu**, M.V. Ramana Murthy and K. Gangadhar******

Abstract

The present study discusses the two dimensional flow of electrically conducting Powell-Erying fluid over a stretching surface in the presence of variable suction/injection. The local similarity solution is used to transform the system of partial differential equations, describing the problem in to a system of highly coupled nonlinear ordinary differential equations. The transformed equations are then solved by the shooting technique combined with the Runge-Kutta-Fehlberg method. The solution is found to be dependent on five governing parameters including the magnetic field parameter, the power-law fluid index, the sheet velocity exponent, the suction/blowing parameter, and the generalized Prandtl number. A systematical study is carried out to illustrate the effects of these major parameters on the sheet surface temperature, fluid temperature distributions in the boundary layer, the skin friction coefficient and the local Nusselt number.

Keywords: *stretching sheet, MHD, Powell-Erying fluid, variable suction or injection.*

---

* Department of Mathematics & Humanities, Chaitanya Bharathi Institute Of Technology, Hyderabad-75, Telangana, India. *Email: suresh.pallerla000@gmail.com*

** Department of Humanities & Sciences, Keshav Memorial Institute Of Technology, Hyderabad, Telangana, India. *Email: nlbhikshu@gmail.com*

*** Department of Mathematics & Computer Science, Osmanaia University, Hyderabad -7, Telangana, India. *Email: mv.rm50@gmail.com*

**** Department of Mathematics, Acharya Nagarjuna University, Ongole, Andhra Pradesh - 523001, India

Nomenclature:

k- Thermal conductivity (W/m K)

c_p – Specific heat at constant pressure (J/kg K)

f- Dimensionless stream function

u-Velocity component in x-direction- (m/s)

v- Velocity component in y-direction-(m/s)

x-Cartesian coordinate in horizontal direction-(m)

T- Temperature of the fluid-(^oC)

T_w – Temperature at the stretching surface

T_∞ - Ambient fluid temperature

$u_w(x)$ –Stretching velocity

λ & δ Material fluid parameters

M-Magnetic parameter

Sc-Schmidt number

Re_x- Local Reynolds number Greek symbols

α – Thermal diffusivity -(m^2/s)

μ - Dynamic viscosity (N s/m)

ρ - Fluid density (kg/m^3)

T_w- Wall shear stress

η - Similarity variable

$\upsilon = \dfrac{\mu}{\rho}$ *- Kinematic viscosity of the fluid*

$\Gamma -$ *Time dependent material constant*

θ - Non-dimensional temperature subscript

w-Condition at the surface

∞-Condition at infinity super script

' -Differentiation with respect to η

1. INTRODUCTION

The applications of Non-Newtonian fluids are very wide and they are mostly useful in processing of food, heat exchangers, reactor cooling, biomedical processes, Nuclear fuel slurries, liquid metals ,alloys, plasma, mercury, heavy oil and greases lubrications, paper coatings, extracting of polymers and many more. The bio fluids, such as, saliva, blood samples and DNA are generally analysed by BIOMEMS devices, but these fluids cannot be treated as Newtonian fluids. The behaviour of these fluids can be described by adopting Cauchy momentum equation with a proper constitutive law as Navier-stokes equation fails in this aspect ,Non-Newtonian fluids mathematical formulation is very complex. The second grade, Maxwell, oldroyd-B and power law models are the frequently considered Non-Newtonian models. Fluids steady and unsteady flow contexts and their behavior together with mathematical models can be found in Ref [1-7]. The Powell-Eyring model certainly has considerable edge over there Non-Newtonian fluid models it is designed from kinetic theory of liquids rather than empirical relation and reduces to Newtonian behavior for low and high shear rates.

First, it is derived from kinetic theory of fluids and can be correctly reduced Newtonian behavior for low and high shear rates. The flow of Powell-Eyring model numerically through asymptotic boundary conditions was examined by Patel and Timol [8] Hayat et al [9] studied the steady flow of a Powell-Eyring fluid over a moving surface with convective boundary conditions. Rosca and Pop[10] presented flow and heat transfer of Powell-Eyring fluid over shrinking surface in a parallel free stream.

The flow of a fluid over a stretching surface has significant polymer-industry applications such as, glass blowing, casting and spinning of fibres incessantly which involve the flow owing to stretching surface. Classical solution for the boundary layer flow of viscous fluid over a sheet moving with varying velocity linearly with distance from a fixed point was provided by Crane [11]. This work has been adopted for stretching flows in distinct configurations Mukhopadhay [12] analyzed the slipping effects on MHD Boundary layer flow by stretching a sheet exponentially with blowing or suction and thermal radiation. Bhikshu et.al [13] investigated the effects of Magnetohydrodynamics on the Peristaltic flow of fourth grade fluid in an inclined channel with permeable walls. Bhattacharya et al [14] have investigated thermal radiation effects on micropolar fluid flow and heat transfer over a porous stretching sheet. Turky ilmazoglu [15] investigated exact solutions for 2-Dimensional laminar flow over a continuously stretching or shrinking sheet in an electrically conducting quiescent couple stress fluid. Turky ilmazoglu [16] studied A note has been presented on micro polar fluid and that transfer over a porous shrinking sheet, Sheikholeslami et al [17] investigated the effect of heat transfer in flow of Nano fluids over a permeable stretching wall in a porous medium nano fluid in a rotating system was analyzed by Sheikholeslami and Ganji [18].

Bhikshu et al [19] studied the peristaltic flow of a conducting Williamson fluid in a vertical asymmetric channel with heat transfer through porous medium. The heat effects generation / absorption on stagnation point flow of nano fluid over a surface with convective boundary was discussed by Alsaedi et al [18]. The MHD stagnation point flow of nano fluid towards a stretching sheet was a analyzed by

Ibrahim et al [20]. Malvandi et al [21] analyzed the effect of slip on unsteady stagnation point flow of nano fluid over a stretching sheet.

Most of the chemically reacting systems include both homogenous and heterogeneous reactions, found in combustion, catalysis and biochemical systems. Chaudhary and Merkin [22] have considered a simple model for homogeneous-heterogeneous reactions in boundary layer flow in which the bulk homogeneous reaction is assumed to be given by isothermal cubic autocatalator kinetics and the heterogeneous surface reaction by first order kinetics. Bachok et al [23] investigated stagnation point flow over a stretching sheet with homogenous and heterogeneous reactions. Homogenous and heterogeneous reactions in a nanofluid flow due to a porous stretching sheet have been investigated by Kameswaran et al [24].

The present study analyses the homogeneous-heterogeneous reactions in a flow of powell-eyring fluid over a stretching sheet. This problem is modeled first and then solved by homotopy analysis method [25−32]. The distinct parameters behavior has been analyzed graphically.

2. MATHEMATICAL FORMULATION:

We consider a steady two-dimensional incompressible flow of Powell-Eyring fluid. We have considered a simple model for both homogeneous and heterogeneous reactions, involving two chemical species A and B in boundary layer flow. For the homogeneous reaction we took isothermal cubic autocatalytic reaction, given schematically by [23]

$$A + 2B \rightarrow 3B, rate = k_1 ab^2 \tag{1}$$

While on the catalyst surface we have the single isothermal first order reaction:

$$A \rightarrow B, rate = k_s a \tag{2}$$

Where a and b are concentrations of chemical species A and B, respectively; and k_1 and k_s are the constants. The stress tensor in an Powell-Eyring model is

$$T_{ij} = \mu \frac{\partial u_i}{\partial x_j} + \frac{1}{\beta} sinh^{-1}\left(\frac{1}{c}\frac{\partial u_i}{\partial x_j}\right) \tag{3}$$

Where μ is the dynamic viscosity; β and c are the material fluid parameters. Considering

$$sinh^{-1}\left(\frac{1}{c}\frac{\partial u_i}{\partial x_j}\right) \cong \frac{1}{c}\frac{\partial u_i}{\partial x_j} - \frac{1}{6}\left(\frac{1}{c}\frac{\partial u_i}{\partial x_j}\right)^3, \left|\frac{1}{c}\frac{\partial u_i}{\partial x_j}\right| \leq 1 \tag{4}$$

A Uniform magnetic field is applied normal to the sheet the magnetic Raynolds number is assumed to be small so that the induced magnetic field can be neglected.

The governing boundary layer equations are

$$\frac{\partial u}{\partial x}+\frac{\partial v}{\partial y}=0 \tag{5}$$

$$u\frac{\partial u}{\partial x}+v\frac{\partial u}{\partial y}=\left(v+\frac{1}{\rho\beta c}\right)\frac{\partial^2 u}{\partial y^2}-\frac{1}{2\rho\beta c^3}\left(\frac{\partial u}{\partial y}\right)^2\frac{\partial^2 u}{\partial y^2}-\delta\frac{\beta_0^2}{\rho}u \tag{6}$$

$$u\frac{\partial a}{\partial x}+v\frac{\partial a}{\partial y}=D_A\frac{\partial^2 a}{\partial y^2}-k_1ab^2 \tag{7}$$

$$u\frac{\partial b}{\partial x}+v\frac{\partial b}{\partial y}=D_B\frac{\partial^2 b}{\partial y^2}+k_1ab^2 \tag{8}$$

Where *u* and *v* are the velocity components along the *x*-and *y*-direction, respectively; $v = \mu/\rho$ is the kinematic viscosity and ρ is the fluid density. D_A and D_B are the respective diffusion coefficients. The boundary conditions set for Eqs. (5)−(8) are:

$$u=U_w x, v=V_w,\ D_A\frac{\partial a}{\partial y}=k_s a\ , D_B\frac{\partial b}{\partial y}=-k_s a \text{ at } y=0$$

$$u\to 0\ , a\to a_0, b\to 0 \text{ as } y\to\infty \tag{9}$$

Where U_w and a_0 are the constants, V_w is the suction/injection coefficient

We define the following transformations:

$$\psi=(U_w v)^{\frac{1}{2}}xf(\eta)\ , g(\eta)=\frac{a}{a_0}\ , h(\eta)=\frac{b}{a_0}\ , \eta=\left(\frac{U_w}{v}\right)^{\frac{1}{2}}y \tag{10}$$

Where ψ is the stream function defined by $u = \partial\psi/\partial y$ and $v = -\partial\psi/\partial x$. Substituting Eq. (10) into Eqs. (5)−(9), we obtain the following ordinary differential equations:

$$(1+\lambda)f'''-f'^2+ff''-\lambda\delta f''^2f'''-\mu f'=0 \tag{11}$$

$$\frac{1}{S_c}g''+fg'-Kgh^2=0 \tag{12}$$

$$\frac{\lambda}{S_c}h''+fh'+Kgh^2=0 \tag{13}$$

where primes denote differentiation with respect to η, λ and δ are the material fluid parameters, S_c is the Schmidt number, K is the measure of the strength of the homogeneous reaction, λ is the ratio of the diffusion coefficients.

The suction or injection Parameter

$$f_w=-\frac{V_w}{U_w v}$$

The Magnetic Parameter

$$\mu=\frac{\sigma\,\beta_0^2}{\rho V_w}$$

These quantities have following definitions

$$\lambda = \frac{1}{\mu\beta c}, \delta = \frac{U_w^3 x^2}{2c^2 v}, S_c = \frac{v}{D_A}, K = \frac{k_1 a_0^2}{U_w}, \beta = \frac{D_B}{D_A} \tag{14}$$

The boundary conditions in eqn (9) become

$$\begin{cases} f(0) = f_w, f'(0) = 1, f'(\eta) \to 0 \; as \; \eta \to \infty \\ g'(0) = K, g(0)\beta h'(0) = -K_s h(0), g(\eta) \to 1 \\ h(\eta) \to 0 \text{ as } \eta \to \infty \end{cases} \tag{15}$$

where K_S measures the strength of the heterogeneous reaction.

Take β=1, we have

$$g(\eta) + h(\eta) = 1 \tag{16}$$

And eqs (12) and (13) give

$$\frac{1}{S_c} g'' + f g' - K g(1-g)^2 = 0 \tag{17}$$

The subjected boundary conditions set are

$$g'(0) = K_s g(0), g(\eta) \to 1 \text{ as } \eta \to \infty (18)$$

Therefore, we have to solve eqs (11) and (17) along with the boundary conditions (15) and (18)

3. SOLUTION OF THE PROBLEM

The above Eqs. (6) and (7) along with the boundary conditions are solved by converting them to an initial value problem. We set

Magnetic field strongly influenced the velocity boundary layer and opposite for concentration boundary layer

$$f' = z, z' = p$$

$$p' = \frac{1}{1 + \lambda - \lambda\delta p^2}(z^2 - fp + \mu z)$$

$$g' = q$$

with the boundary conditions

Velocity and concentration boundary layer are decreased suction.

$$q' = S_c(Sg(-g)^2 - fq)$$

$$f(0) = f_w, z(0) = 1, q(0) = K_s g(0)$$

Magnetic parameter M or material fluid parameter λ, Schmidt number S_c, measure of the strength of the homogenous reaction parameter K_s.

In order to integrate (10) and (11) as an initial value problem, one requires a value for p(0), that is $f''(0)$ and $q(0)$, that is, $g'(0)$ no such values are given at the boundary. The suitable guess values for $f''(0)$ and $h'(0)$ are chosen and then integration is carried out. Comparing the calculated values for f' and g at $\eta = 10$ (say) with the given boundary conditions $f'(10) = 1$ and g(10)=0 and adjusting the estimated values $f''(0)$ and $g'(0)$ we apply the fourth order classical Runge-Kutta method with step-size h=0.01. The above procedure is repeated until we get the converged results within a tolerance limit of 10^{-5}.

4. RESULTS AND DISCUSSION

In order to analyze the results, numerical computation has been carried out using the method described in the previous section for various values of magnetic parameter M material fluid parameter λ, Schmidt number Sc measure of strength of the homogeneous reaction parameters K (Ks) For illustration of the results, numerical values are plotted in Figs 1 to 12.

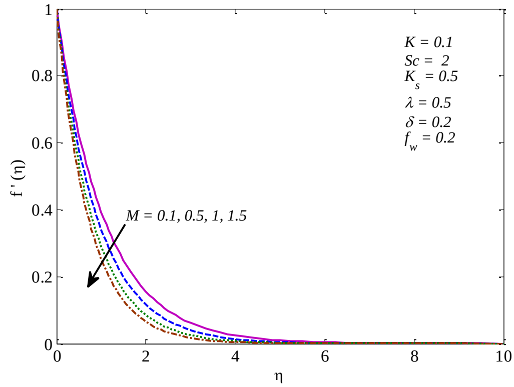

Figure 1: Velocity profile $f'(\eta)$ for different values of M

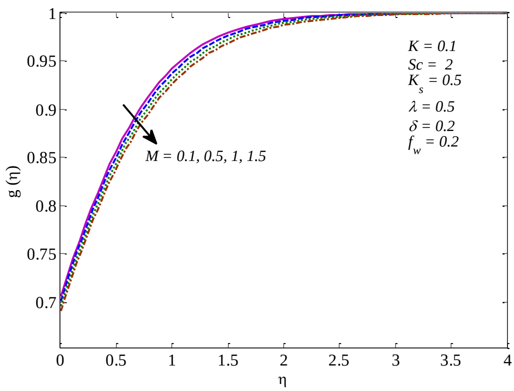

Figure 2: Concentration profile $g(\eta)$ for different values of M

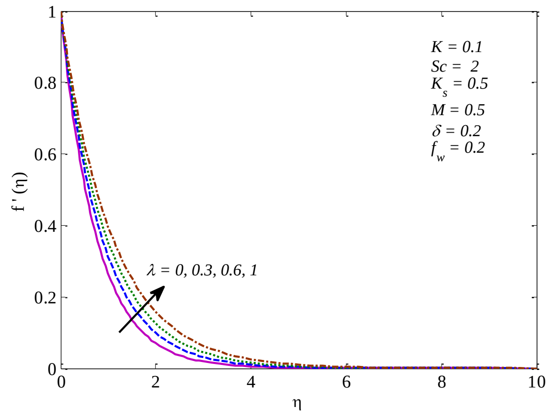

Figure 3: Velocity profile $f'(\eta)$ for different values of λ

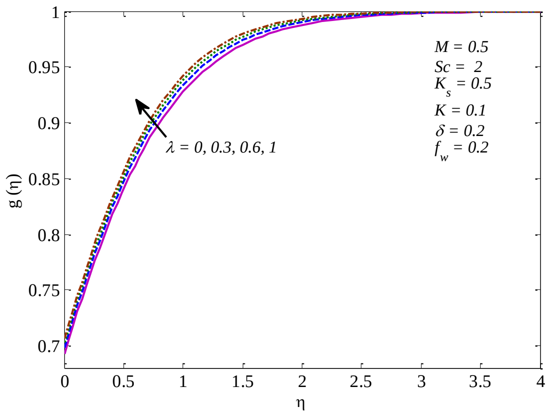

Figure 4: Concentration profile $g(\eta)$ for different values of λ

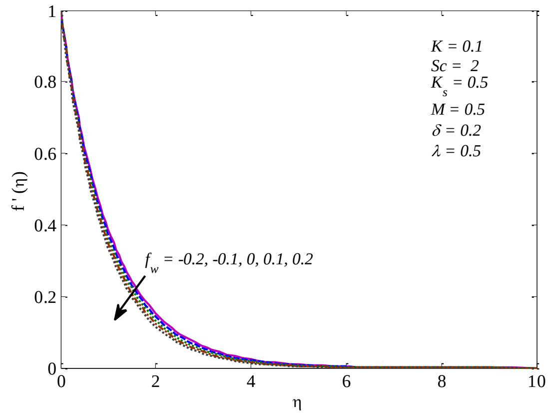

Figure 5: Velocity profile $f'(\eta)$ for different values of f_w

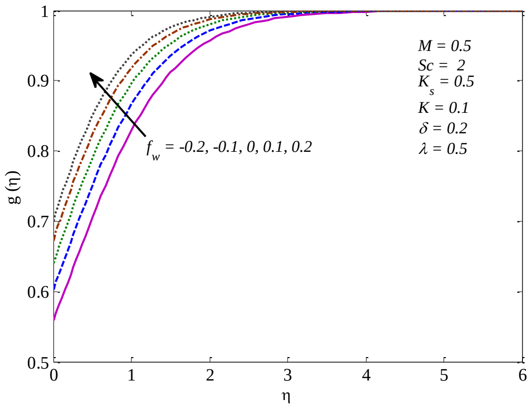

Figure 6: Concentration profile $g(\eta)$ for different values of f_w

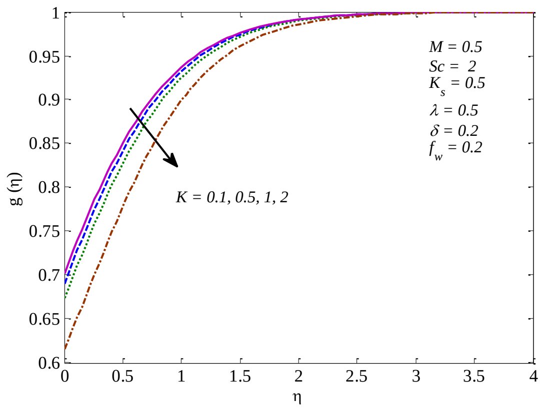

Figure 7: Concentration profile $g(\eta)$ for different values of K

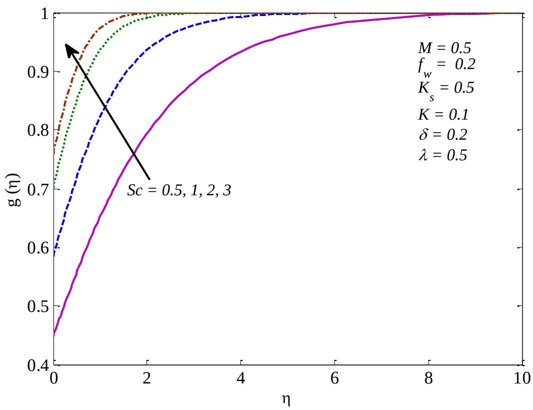

Figure 8: Concentration profile $g(\eta)$ for different values of Sc

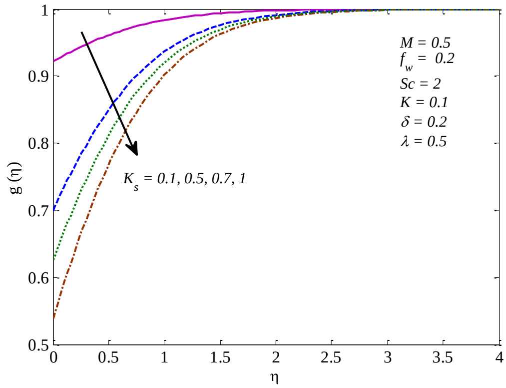

Figure 9: Concentration profile $g(\eta)$ for different values of K_s

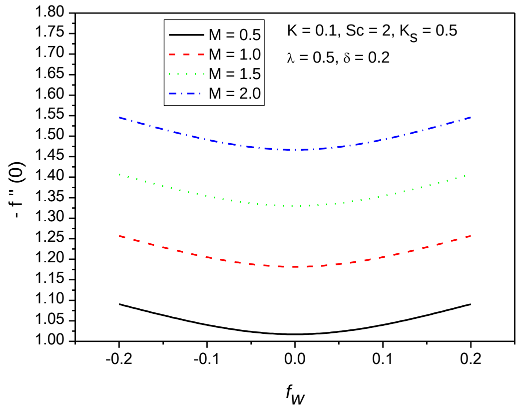

Figure 10: Skin-friction coefficient $-f''(0)$ for different values of M & f_w

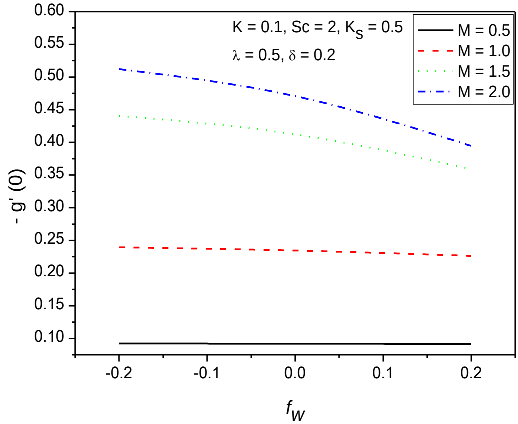

Figure 11: Sherwood number $-g'(0)$ for different values of M & f_w

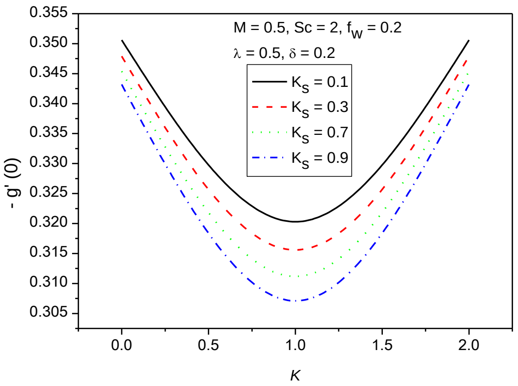

Figure 12: Sherwood number $-g'(0)$ for different values of K_s & K

Figure 1 shows that velocity distribution for different values of magnetic parameters M. It is clearly observed that velocity profile decreases with increasing in M values due to increment of magnetic field strength, a resistive type force called Lorentz force associated with the aligned magnetic field makes the boundary layer thinner and also the magnetic field lines.

Figure 2 demonstrated the effect of M on concentrated profile it is noticed that temperature profile increases with increasing M.

Figure 3 and 4 shows the effect of material parameter λ on velocity and concentration profiles respectively. It is clear that velocity profile and concentration profile increases with increase λ.

Figure 5 and 6 shows the effect of suction/injection parameter the on the velocity and concentration distribution. It is observed that the velocity profiles decreases with rise in f_w whereas concentration profiles increases with a rise in f_w. The concentration profiles for different values of homogeneous parameter K is shown in Figure 7. It is noticed that the concentration profiles decrease with an in increase in K. It is also observed that concentration profile increases with increase Schmidt number S_c.

Figure 9 shows that the effect of K_s on concentration. From this figure we observed that concentration decreases with an increasing in K_s.

Figure 10 shows that skin friction of $f''(0)$ decreases for nagatives of f_w and increases for positive values of f_w.

Figure 11 demonstrate that the Sherwood $g^I(0)$ is decreases as suction / injection Coefficient f_w increases.

Figure 12 shows that The effect of K for different values of K_s .From this figure we observe that the sherwood decreases as K increases from 0 to 1and increases as K increases as K increases from 0 onwards.

5. CONCLUSIONS

1. The present study discusses the two dimensional flow of electrically conducting Powell-Eyring fluid over a stretching surface in the presence of variable suction/injection. The local similarity solution is used to transform the system of partial differential equation describing the problem into a system of highly coupled non-linear ordinary differential equations. The transformed equations are then solved by shooting technique combined with Runge-kutta fourth order method.

2. For different values of magnetic parameters M, it is clearly observed that velocity profile decreases with an increasing values of M due to increment in magnetic field strength

3. It is noticed that temperature profile increases with increase in M.

4. Velocity profile and concentration profile increases with in λ.

Table 1: Comparison of Skin-friction coefficient $-f''(0)$ with the available results in literature for different values of M when $\lambda = K = K_s = 0$.

M	$-f''(0)$		
	Present study	*Chen*	*Andersson et al. [14]*
0.0	1.000000	1.00000	1.000
0.5	1.224745	1.22475	1.225
1.0	1.414214	1.41421	1.414
1.5	1.581139	1.58114	1.581
2.0	1.732051	1.73205	1.732

References

[1] Turkyilmazoglu m. Dual and triple solutions for MHD slip flow of non-Newtonian fluid over a shrinking surface [J]. Computers & Fluids, 2012, 70: 53−58.

[2] Fetecau C, Jamil m, Mahmood A. Flow of fractional Maxwell fluid between coaxial cylinders [J]. Archive of Applied Mechanics, 2011, 81: 1153−1163.

[3] Yin C, Niu J, Fu C, Tan W C. Thermal convection of a visco elastic fluid in a fluid-porous system subjected to horizontal plane couette flow [J]. International Journal of Heat and Fluid Flow, 2013, 44: 711−718.

[4] Makinde O D, Chinyoka T, Rundora L. Unsteady flow of a reactive variable viscosity non-Newtonian fluid through a porous saturated medium with asymmetric convective boundary conditions [J]. Computers & Mathematics with Applications, 2011, 62:3343−3352.

[5] Ellahi R. The effects of MHD and temperature dependent viscosity on the flow of non Newtonian nanofluid in a pipe: Analytical solutions [J]. Applied Mathematical Modelling, 2013, 37: 1451−1467.

[6] Rashidi M M, Pour S A M, Abbasbandy S. Analytic approximate solutions for heat transfer of a micropolar fluid through a porous medium with radiation [J].

Communications in Nonlinear Science and Numerical Simulation, 2011, 16: 1874−1889.

[7] Awais M, Hayat T, Alsaedi A, Asghar S. Time-dependent three-dimensional boundary Layer flow of a Maxwell fluid [J]. Computers & Fluids, 2014, 91: 21−27.

[8] Patel M, Timol M G. Numerical treatment of Powell-Eyring fluid flow using method of Satisfaction of asymptotic boundary conditions (MSABC) [J]. Applied Numerical Mathematics, 2009, 59: 2584−2592.

[9] Hayat T, IQBAL Z, Qasim M, ObaidaT S. Steady flow of an Eyring Powell fluid over a Moving surface with convective boundary conditions [J]. International Journal of Heat and Mass Transfer, 2012, 55: 1817−1822.

[10] Rosca A V, Pop I. Flow and heat transfer of Powell-Eyring fluid over a shrinking surface in a parallel free stream [J]. International Journal of Heat and Mass Transfer, 2014, 71: 321−327.

[11] Crane L J. Flow past a stretching plate [J]. Z Angew Math Physk, 1970, 21: 645−647.

[12] MukhopadhyaY S. Slip effects on MHD boundary layer flow over an exponentially stretching sheet with suction/blowing and thermal radiation [J]. Ain Shams Engineering Journal, 2013, 4: 485−491.

[13] Bhikshu N. L. The effects of Magnetohydrodynamics on the Peristaltic flow of fourth grade fluid in an inclined channel with permeable walls. Jr. of Chemical, Biological and Physical Sciences (JCBPS); Oct. 2015, Vol. 5, No. 4; 4251-4268.

[14] Bhattacharyya K, MukhopadhyaY S, Layek G C, Pop I. Effects of thermal radiation on micropolar fluid flow and heat transfer over a porous shrinking sheet [J]. International Journal of Heat and Mass Transfer, 2012, 55: 2945−2952.

[15] Turkyilmazoglu M. Exact solutions for two-dimensional laminar flow over a continuously stretching or shrinking sheet in an electrically conducting quiescent couplestress fluid [J]. International Journal of Heat and Mass Transfer, 2014, 72: 1−8.

[16] Turkyilmazoglu M. A note on micropolar fluid flow and heat transfer over a porous shrinking sheet [J]. International Journal of Heat and Mass Transfer, 2014, 72: 388−391.

[17] Sheikholeslami M, Ellahi R, Ashorynejad H R, Donairry G, Hayat T. Effects of heat transfer in flow of nanofluids over a permeable stretching wall in a porous medium [J]. Journal of Computational and Theoretical Nanoscience, 2014, 11: 486−496.

[18] Sheikholeslami M, Ganji d D. Three dimensional heat and mass transfer in a rotating system using nanofluid [J]. Powder Technology, 2014, 253: 789−796.

[19] Bhikshu N. L. Peristaltic Flow of a Conducting Williamson Fluid in a Vertical Asymmetric Channel with Heat Transfer through Porous Medium. IPASJ International Journal of Mechanical Engineering (IIJME). Volume 3, Issue 8, August 2015, 27-38.

[20] Alsaedi A, Awais M, Hayat T. Effects of heat generation/ absorption on stagnation point flow of nanofluid over a surface with convective boundary conditions [J].

Communications in Nonlinear Science and Numerical Simulation, 2012, 17: 4210−4223.

[21] Ibrahim W, Shankar B, Nandeppanavar m M. MHD stagnation point flow and heat transfer due to nanofluid towards a stretching sheet [J]. Inernational Journal of Heat and Mass Transfer, 2013, 56: 1−9.

[22] Malvandi A, Hedayati F, Ganji d D. Slip effects on unsteady stagnation point flow of a nanofluid over a stretching sheet [J]. Powder Technology, 2014, 253: 377−384.

[23] Chaudhary M A, Merkin J H. A simple isothermal model for homogeneous-heterogeneous reactions in boundary layer flow [J]. I equal diffusivities. Fluid Dynamics Research, 1995, 16: 311−333.

[24] Bachok N, Ishak A, Pop I. On the stagnation-point flow towards a stretching sheet with homogeneous-heterogeneous reactions effects [J]. Communications in Nonlinear Science and Numerical Simulation, 2011, 16: 4296−4302.

[25] Kameswaran P K, Shaw S, Sibanda P, MURTHY P V S N. Homogeneous-Heterogeneous reactions in a nanofluid flow due to a porous stretching sheet [J]. International Journal of Heat and Mass Transfer, 2013, 57: 465−472.

[26] Liao S J. On the relationship between the homotopy analysis method and Euler transform [J]. Communications in Nonlinear Science and Numerical Simulation, 2010, 15: 1421−1431.

[27] Zheng L, Niu J, Zhang X, Gao Y. MHD flow and heat transfer over a porous shrinking surface with velocity slip and temperature jump [J]. Mathematical and Computer Modelling, 2012, 56: 133−144.

[28] Shehzad S A, Alsaedi A, Hayat T, Alhuthali M S. Thermophoresis particle deposition in mixed convection three-dimensional radiativeflow of an Oldroyd-B fluid [J].Journal of Taiwan Institute of Chemical Engineers, 2014, 45: 787−794.

[29] Awais M, Hayat T, Alsaedi A, Asghar S. Time-dependent three-dimensional boundary layer flow of a Maxwell fluid [J]. Computers & Fluids, 2014, 91: 21−27.

[30] Abbasbandy S, Shivanian E. Predictor homotopy analysis method and its applicationto some nonlinear problems [J]. Communications in Nonlinear Science and Numerical Simulation, 2011, 16: 2456−2468.

[31] Arqub O A, El-ajou A. Solution of the fractional epidemic model by homotopy analysis method [J]. Journal of King Saud University, 2013, 25: 73−81.

[32] Turkyilmazoglu M. A note on homotopy analysis method [J]. Applied Mathematics Letters, 2010, 23: 1226−1230.